Journal of Neuroscience Methods 201 (2011) 124–130

Contents lists available at ScienceDirect

Journal of Neuroscience Methods

journal homepage: www.elsevier.com/locate/jneumeth

Brain activity during stepping: A novel MRI-compatible device

Christoph Hollnagel[a,*], Mike Brügger[a,b], Heike Vallery[a], Peter Wolf[a], Volker Dietz[c], Spyros Kollias[b], Robert Riener[a,c]

[a] Sensory-Motor Systems (SMS) Lab, Institute of Robotics and Intelligent Systems (IRIS), ETH Zurich, Zurich, Switzerland
[b] Institute for Neuroradiology, University Hospital of Zurich, Zurich, Switzerland
[c] Spinal Cord Injury Center, Balgrist University Hospital, Zurich, Switzerland

ARTICLE INFO

Article history:
Received 19 May 2011
Received in revised form 20 July 2011
Accepted 21 July 2011

Keywords:
fMRI
MR robotics
Gait-like movements
Foot loading
Therapy assessment
Head fixation

ABSTRACT

Little is known about the impact of supraspinal centers on the control of human locomotion. Analyzing brain activity can help to clarify their impact and to improve the effects of locomotor training. A fMRI-compatible pneumatic robotic device is presented that can generate freely programmable, highly repetitive periodic active and passive leg movements comprised by hip, knee, and ankle joint displacements. Forces of up to 400 N can be applied to each foot while the subject is lying in a supine position. Magnetic interference of the device with the magnetic field of the scanner is measurable, but does not affect the image quality as obtained by a usual image analysis procedure. In a first experiment, brain activity of one healthy subject was acquired during nine different gait-like movement conditions. Brain activity in the somatosensory and motor function related areas increased more when the subject actively moved the legs than when the legs were passively moved by the device. In almost all conditions, mean head motion could be limited to 2 mm within the duration of one fMRI scan by a specifically developed head and trunk fixation system. Based on these results, it is concluded that our device will significantly contribute to a better understanding of human locomotor control and related therapeutic effects in spinal cord injured and stroke patients, and thereby, to improve training approaches.

© 2011 Elsevier B.V. All rights reserved.

1. Introduction

A dysfunction of neuronal circuits relevant for locomotion develops over time when spinal cord injured (SCI) subjects remains immobile after an injury (Dietz et al., 2009). Gait training with robotic gait orthoses like the LOKOMAT (Hocoma AG, Switzerland, Colombo et al., 2000) has been proposed to prevent such a neuronal dysfunction.

Currently, neither the underlying mechanism of dysfunction, nor the therapeutic effects of gait training on spinal and supraspinal neuronal circuits are fully understood. Knowledge about these mechanisms would help to improve the therapeutic efficacy of gait training. While training effects on spinal neuronal centers have been described (Dietz et al., 2002), training effects on supraspinal centers are almost unknown. A better insight view might be achieved by the assessment of the brain activity during gait or lower limb movements. This can help to recognize the significance of specific brain regions in the recovery of function and the effects of specific training regimes on brain centers in CNS injured subjects.

An established method to assess brain activity is functional magnetic resonance imaging (fMRI). It is a non-invasive technique featuring high spatial resolution of brain activity without any serious contraindications. In combination with a MR-compatible robotic device enabling gait-like movements in a repetitive and controlled manner, fMRI can measure brain activity during gait-like movements. Inserting a robotic device into the magnetic resonance scanner environment raises several challenges and constrains to its design: First, the device should neither disturb the imaging process nor harm the technical scanner environment or any subject in its vicinity. Second, the magnetic field of the scanner should also not affect the functionality of the device. In order to apply a robotic device that enables gait-like movements in the scanner, further challenges have to be taken into account: Third, the posture in the supine yields unnatural gravitational effects to the feet (missing ground reaction load) and the trunk (additional contact forces from the bench to the back). Fourth, due to the restricted space inside the scanner, leg movements have to be simplified compared to physiological gait. However, the pattern must remain similar in several key characteristics in order to lead to a locomotor pattern in the relevant leg muscles (Dietz et al., 2002). These key features concern the coordinated trajectories of ankle, knee and hip joints in the sagittal plane, as well as foot contact forces (Dietz and Duysens, 2000; Dietz et al., 1992). Fifth, head motion must be limited, to assure that image quality is not affected by movement artifacts.

Brain activity during multi-joint leg movements has been investigated with fMRI, e.g. during cycling (Christensen et al., 2000;

* Corresponding author. Tel.: +41 446327353.
E-mail address: hollnagel@mavt.ethz (C. Hollnagel).

0165-0270/$ – see front matter © 2011 Elsevier B.V. All rights reserved.
doi:10.1016/j.jneumeth.2011.07.022

Mehta et al., 2009). However, these approaches suffered from excessive head motion, and they did not consider appropriate foot loading. Several other groups investigated brain activity during simplified gait-related movements. They concentrated on isolated joint movements, like ankle or knee flexion/extension (Ciccarelli et al., 2005; Dobkin et al., 2004; Luft et al., 2005, 2002; MacIntosh et al., 2004; Sahyoun et al., 2004), or imagination of walking (Bakker et al., 2007a; Jahn et al., 2004; Malouin et al., 2003; Sahyoun et al., 2004). However, coordinated movement of several joints is important to obtain a realistic gait pattern and activate gait-like muscle activity in the legs (Ivanenko et al., 2002; Kawashima et al., 2005), with the associated nervous representations in the brain. Brain activity during natural gait has been studied with positron emission tomography (PET) and single photon emission computed tomography (SPECT) (Fukuyama et al., 1997; Hanakawa et al., 1999; la Fougère et al., 2010). However, walking on a treadmill and acquiring brain activity was not concurrently but consecutively performed. Furthermore, assessments of brain activity by PET and SPECT require administration of a contrast medium, which can be harmful. Furthermore, also near-infrared spectroscopy (NIRS) has been applied to assess brain activity during gait (Miyai et al., 2006, 2001). In contrast to PET and SPECT, this method allows concurrent acquisition of brain activity during gait without contrast medium, but it has a rather poor spatial resolution (Bakker et al., 2007b).

To overcome the above-mentioned limitations, we constructed a Magnetic Resonance Compatible Stepper (MARCOS), which allows gait-like movements with the corresponding ground reaction forces inside a MR scanner without being affected by the magnetic field of the scanner and without affecting the imaging quality. Both active and passive modes are possible, i.e. the hip, knee, and ankle joints are either moved actively by the subject himself, or they are passively moved by the device. During these movements, the corresponding brain activity can be recorded by the MR scanner.

It is hypothesized that activity in lower limb related regions of the motor-sensory network as primary sensory (S1), primary motor (M1) and supplementary motor (SMA) areas is increased during movements with MARCOS. Additionally, these activity patterns should be more pronounced the more the subject is challenged.

This paper presents the design of MARCOS, its influence on the MR-environment, and first results obtained by a preliminary fMRI study with one healthy subject. FMRI experiments were performed with a single subject, thus, no general conclusions are drawn about brain activity during movements with MARCOS. Instead, the focus of this report is to assess the feasibility of MARCOS.

2. Methods

2.1. MARCOS design

Studies about body weight supported treadmill walking showed that electromyographic activity of leg muscles and angular trajectories at the hip and knee remain physiological as long as they incorporate ground reaction forces at least in the magnitude of half the body weight (Ivanenko et al., 2002; Kamibayashi et al., 2009) and sufficient hip joint excursions (Dietz et al., 2002). In addition, leg muscle EMG activity is amplified if both legs move in an alternating manner (Kawashima et al., 2005). Accordingly, MARCOS can move the legs in an alternating manner and can generate forces of up to 400 N at the foot sole (Fig. 1, right). The chosen kinematics, featuring one degree of freedom for each leg, enable a movement pattern that is comparable to periodic movements when stepping on the spot. Pneumatic actuation was chosen because it allows an MR-compatible design while featuring high maximum forces and good control performance (Yu et al., 2008). Furthermore, pneumatic actuators are compliant and can easily be switched to a force-free state by connecting both cylinder chambers to the atmosphere, which is important to guarantee safety. All ferromagnetic parts in the piston were replaced by custom-made pieces manufactured from aluminum and brass.

Each knee and foot of the subject is strapped to a modified pneumatic cylinder (DNC 40-320-P-K10-S11 (knee), DNC 32-350-P-K10-S11 (foot) Festo, Esslingen am Neckar, Germany). The vertical cylinder at the knee induces forces that move the knee up and down. At each leg, these forces are guided through two orthopedic cuffs, one proximally and one distally, placed around the knee and connected by a hinge joint. These cuffs are used in order to optimally distribute the force to a large contact surface, thus, reducing contact pressure. The axis of the hinge joint is in rough alignment with the anatomical axis of the knee. The pneumatic cylinder at the foot induces a force in such way that the foot moves along the linear guide. This force is guided through the foot insole in order to generate the appropriate afferent input (Fig. 1, left and right).

The position and orientation of the linear guide at each foot can be adjusted to vary hip and knee joint trajectories. At the hip, flexion between 0° and 40° is possible (during gait it varies between 15° extension and 20° flexion (Perry et al., 1992)). At the knee, flexion can range from 0° to 60° at the knee (during gait between 0° and 60° flexion). The foot orientation is fixed so that the angular displacements at the ankle range between 45° and 90° (during gait between -20° and 10°) (Fig. 1, right). The desired input signal is always sinusoidal, to reduce jerk and, thus, head motion.

The cylinders connected to the knees are controlled by proportional flow valves, while the cylinders connected to the feet are controlled by pressure-control valves and a proportional multi-way valve (Fig. 2). For safety reasons, the proportional way valve is always set to a position that produces forces pressing against the foot only (no pulling in negative x-direction, see also Fig. 1, right).

Resistive strain gauges on aluminum substrate serve to record forces. They are attached between each piston and the corresponding orthopedic cuff. The position of each cylinder is measured redundantly by optical encoders (Type MS20, RSF Elektronik AG, Schwerzenbach, Switzerland) with a ceramic scale and one foil potentiometer (MTP L22, Resenso, Ins, Switzerland). Two personal computers are used for signal analysis and control: the sensor evaluation CPU runs Linux, and it processes data from the data acquisition boards. It communicates via Ethernet with the control CPU, which runs Matlab xPC real-time target and executes low-level pneumatic control and high-level gait pattern control.

Several redundant mechanisms are incorporated in order to ensure safety for the subjects: (1) Mechanical stops on each cylinder restrict anatomically inappropriate positions. (2) The position of each cylinder is redundantly measured by two position sensors. Divergent values are detected by the control software, which would launch an emergency stop. (3) Sensors and communication between the sensor evaluation CPU and the control CPU are supervised by the control software. In case of an error, an emergency stop is launched. (4) Watchdog circuits supervise the computers and communication. (5) Emergency stops can be launched by the operator by pressing an emergency switch. (6) In case of an emergency stop (launched by software or manually), all cylinder chambers are connected to the atmosphere by closing the safety valves (Fig. 2). Then, the cylinders can be moved freely and the subject can easily be released from MARCOS.

To minimize interference with the MR scanner, MARCOS only consists of PVC, aluminum, and brass, as these materials are characterized by a low magnetic susceptibility. The region of interest, i.e. the human brain, is more than 1 m away from the nearest metallic part of MARCOS. Movements of metallic parts with relevant electrical conductivity were avoided as much as possible to limit

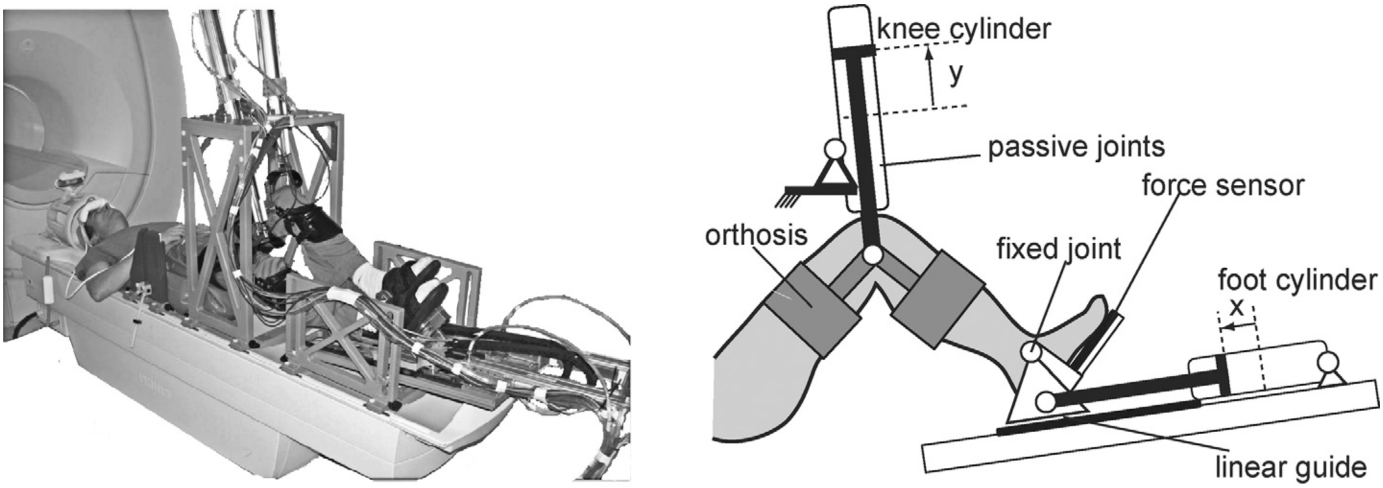

Fig. 1. MARCOS in the fMRI scanner (left), principle sketch of MARCOS (right).

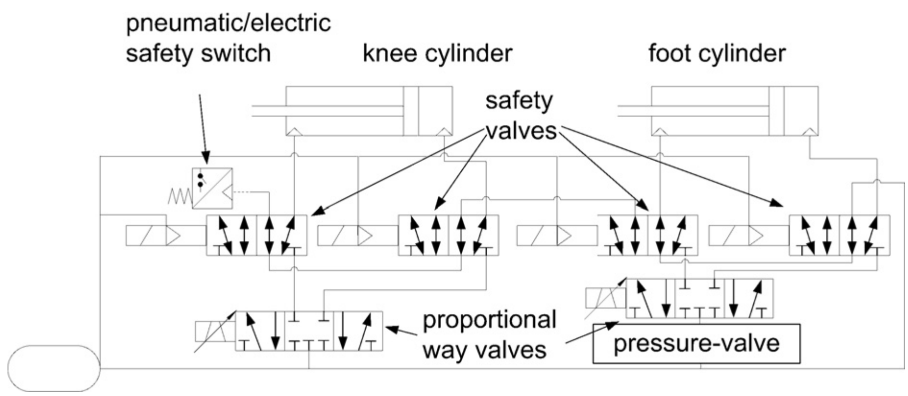

Fig. 2. Pneumatic control layout of MARCOS.

the generation of eddy currents. All sensor signals are collected inside the scanner room, and they are transferred to the control computer via glassfibre cables. The only metallic cable leading into the scanner room is a shielded DC cable for the sensor power supply. The shield of the cable is connected to the shielding of the scanner room, and the DC current is low-pass-filtered.

2.2. Control

The control structure consists of a low-level pneumatics controller and a high-level stepping controller.

The pneumatics controller is responsible of the position of the two knees and the forces applied to the two feet, i.e. four control variables. The controller receives four input signals: Desired mass flow for the knee cylinders, and desired pressure at the foot cylinders. At the feet, an underlying pressure control valve fulfills the task of pressure regulation.

Control of smooth movements with pneumatics in the MR scanner environment is challenging, because the valves must be placed outside of the scanner room. Hence, long tubes (7 m) are required to connect the cylinders inside the scanner room to the valves outside. The compressibility and inertia of air inside the tubes and the softness of the tubes leads to an increased compliance, delay, and low-pass filter effects of the entire system. Furthermore, the magnetic field restricts the choice of materials for the cylinders and bearings, leading to sub-optimal material combinations with increased friction.

Due to these challenges, control with conventional approaches – such as proportional-integral-derivative (PID) and model-based feed-forward control – did not generate satisfactory results in first tests. Hence, an iterative learning controller (Bristow et al., 2006) was implemented. Before any fMRI session, the controller learns an optimal feed-forward sequence for the movements that will be performed during the fMRI measurements. This learning takes place during 20 cycles. From each cycle $k-1$ to cycle k, the controller calculates a four-dimensional feed-forward control signal $u_k(t)$ based on the $(k-1)$-th control output and the $(k-1)$-th four-dimensional error trajectory $e(t)$. The error is pre-multiplied by the 4×4 learning matrix $\mathbf{P}_{ILC}$, and the previous control output u_{k-1} is pre-multiplied by the 4×4 forgetting matrix $\mathbf{Q}$:

$$u_k(t) = \mathbf{Q}u_{k-1}(t) + \mathbf{P}_{ILC}e_{k-1}(t+\Delta t)$$

The diagonal entries of $\mathbf{Q}$ were set to 0.9. The shift Δt of the error trajectory was adjusted to compensate for the reaction time of the system.

Using this underlying force and position control of the pneumatic control loop, high-level controllers execute the desired stepping task for a specific experimental condition. MARCOS can work in a subject-active and in a subject-passive mode. Both modes allow an independent control of the simulated ground reaction force, which is provided by the cylinder at the foot. In subject-active mode, the controller attempts to regulate reaction forces at the knee to zero. In subject-passive mode, MARCOS executes a stiff position control at the knee cylinders. Depending on the current

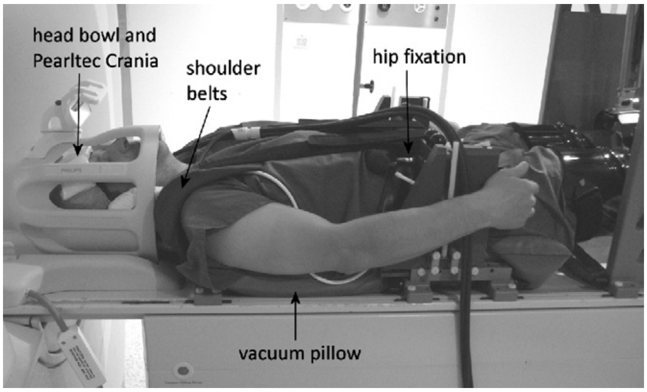

Fig. 3. Fixation applied in the MR scanner.

task, the cylinder at the foot can produce a corresponding cyclic force.

2.3. Head fixation

Image quality is affected by too much head motion. Therefore, head motion in cranial–caudal direction has to be limited to a range of 2 mm over a period of three seconds, i.e. over a period required for a complete functional scan of the head. Head motion up to this value can be corrected by the motion correction algorithm of the Matlab toolbox SPM (statistical parametric mapping).

In several pre-studies, different versions of fixations were tested with respect to comfort, ease of use and effectiveness of head motion suppression. Shoulder belts, a vacuum pillow placed at the back, a custom-made rigid hip fixation, and a custom-made head bowl in combination with the Crania fixation (Pearltec AG, Zurich, Switzerland) were rated as most successful and, thus, applied during fMRI measurements (Fig. 3). The Crania fixation is an inflatable ring that is placed between the head and the head coil. Subjects can regulate the pressure via a small pump, similar to those used for blood pressure measurements. Subjects are asked to use as much pressure as possible without compromising comfort.

2.4. Experimental quantification of influence on the MR environment

The influence on the MR environment was measured by calculating the change of the temporal signal-to-noise ratio of 49 points in the center of an fMRI picture of a phantom (bottle of water). The following conditions were tested as suggested in the literature (Firbank et al., 1999): (i) baseline: MARCOS was outside the scanner room, (ii) connected: MARCOS was mounted on the bench (cables connected), (iii) moving: while mounted on the bench, MARCOS was powered and the actuators moved, and (iv) 2nd baseline: the first condition was repeated.

The measurements were done inside a 3.0-T MR system (Philips Medical Systems, Eindhoven, The Netherlands) combined with an 8-channel SENSE head coil. For functional acquisition, a T2* weighted, single-shot, field echo, EPI sequence of the whole brain with a SENSE factor of 2 was applied to collect signals from 39 contiguous slices (TR = 2 s, TE = 40 ms, flip angle = 82°, FOV = 220 mm × 220 mm, acquisition matrix = 128 × 128, in-plane resolution = 1.7 mm × 1.7 mm, and slice thickness = 3 mm).

To calculate the temporal signal-to-noise ratio tSNR, the values of 49 voxel in the middle of the phantom were measured 20 times. The mean value for each voxel time series was divided by its standard deviation (Yu et al., 2011).

The results were analyzed with a post hoc Kruskal–Wallis statistical test in Matlab (Mathworks Inc., Natiek, MA, USA).

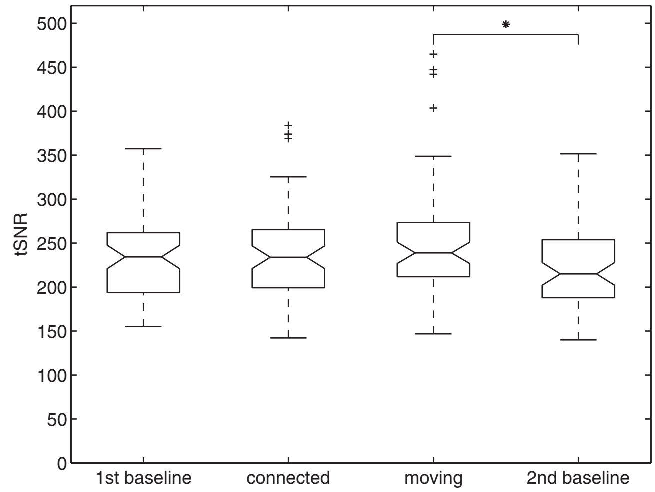

Fig. 4. Temporal signal-to-noise ratio (tSNR) of measurements with MARCOS: no device (1st baseline), cables connected, moving device, and no device (2nd baseline). The asterisk (*) marks the statistical difference of the condition "moving" and "2nd baseline".

2.5. fMRI acquisition and data analysis

2.5.1. fMRI parameters

A first study was carried out at the MR Center of the University and ETH Zurich, using a Philips Achieva 1.5 T MR system with an 8-channel SENSETM head coil. The functional acquisitions used a T2* weighted, single-shot, field echo, echo-planar-imaging sequence of the whole brain (TR = 3 s, TE = 50 ms, flip angle = 82°, FOV = 220 mm × 220 mm, acquisition matrix = 128 × 128, in-plane resolution = 1.7 mm × 1.7 mm, slice thickness = 3.8 mm, and SENSE factor 1.6, resulting in 35 slices). Whole brain anatomical images were acquired using a 3D, T1-weighted, field echo sequence (TR = 20 ms, TE = 4.6 ms, flip angle = 20°, in-plane resolution = 0.9 mm × 0.9 mm, slice thickness = 0.75 mm, and 210 slices).

2.5.2. Task parameters

According to the movement conditions allowed by MARCOS, nine different movement paradigms were applied:

(1) Alternating passive stepping at 0.5 Hz (Alt-pas).
(2) Alternating active stepping at 0.5 Hz (Alt-act).
(3) Passive left leg movement at 0.5 Hz (L-pas).
(4) Passive right leg movement 0.5 Hz (R-pas).
(5) Active left leg movement at 0.5 Hz (L-act).
(6) Active right leg movement at 0.5 Hz (R-act).
(7) Alternating passive stepping at 0.5 Hz with foot loading (0–200 N) (Alt-pas-F).
(8) Alternating active stepping at 0.5 Hz with foot loading (0–200 N) (Alt-act-F).
(9) Alternating passive stepping at 1 Hz without foot loading (Alt-pas-1 Hz).

These movements were applied in one subject (male, 30 years, weight: 72 kg, no neurological or orthopedic problems, signed informed consent) while brain activity was measured. The experiment should serve as a proof of concept, thus, no general conclusions are drawn about brain activity during movements with MARCOS. Ethical approval for this measurement was obtained by the local cantonal ethical committee. Each movement paradigm was executed 30 times for 10 s (five steps for 0.5 Hz), interleaved by a pause of 5 s. The subject was asked to keep the eyes closed and to relax. Before scanning, he got familiar with the movements of the robot and the head and body fixation.

Table 1
Mean head motion during fMRI measurements and its standard deviation (std) during different tasks.

Task	Lateral mean/std (mm)	Rostrocaudal mean/std (mm)	Dorsoventral mean/std (mm)
Alt-pas	0.08/0.07	1.54/0.62	1.25/0.6
Alt-act	−0.28/0.17	−0.05/0.48	−0.63/0.4
L-pas	−0.06/0.05	−0.81/0.28	−2.41/0.80
R-pas	0.06/0.12	0.44/0.79	0.18/0.67
L-act	0.09/0.06	0.1/0.05	−0.23/0.15
R-act	−0.01/0.03	0.31/0.23	0.46/0.3
Alt-pas-F	−1.11/0.3	−1.51/0.78	−8.12/1.81
Alt-act-F	−0.45/0.21	−0.46/0.25	−2.26/0.86
Alt-pas-1 Hz	−0.09/0.14	0.01/0.53	−1.13/0.56

The movement and breaks performed by MARCOS during the block design fMRI measurements, were triggered by the software Presentation (Neurobehavioral Systems, Inc., San Francisco Bay Area, USA) that also labeled the scans with the respective condition.

2.5.3. fMRI analysis

Image processing and analysis were performed using SPM8 (Welcome Department of Cognitive Neurology, London) implemented in MATLAB 7.6/R2008a (Mathworks Inc., Natiek, MA, USA). All functional images were re-aligned to the mean image followed by normalization into the standard stereotactic space using the Montreal Neurological Institute template. Spatial smoothing was performed applying a Gaussian filter of 8 mm full width half max. A first-level statistical analysis was conducted by modeling each single condition in a general linear model using the canonical hemodynamic response function. This data analysis was performed on a single-subject basis, to identify the activated neuronal network involved in the respective movement tasks.

2.5.4. Brain activity patterns: hypothesis

As no comparable literature has been published with respect to cortical underpinnings of gait-like movements, the hypothesis was derived from studies that investigated isolated joint movements (Luft et al., 2002) or imagination of walking (i.e. la Fougère et al., 2010).

Main brain activity in primary and secondary sensorimotor areas, S1, M1, SMA, was expected. Especially when the subject was actively moving the legs, enhanced brain activity was expected within the sensorimotor areas as compared to the passive movements.

3. Results

3.1. Influence on the MR-environment

A post hoc Kruskal–Wallis test showed a significant difference ($p = 0.022$) only for the conditions “moving device” and “2nd baseline” (Fig. 4).

3.2. fMRI measurements

The amplitude of high-frequent head motion during one scan of the fMRI measurements remained below 2 mm for most conditions (Table 1). In task Alt-pas-F, a strong drift during the first scans was detected. Activity in the primary motor/sensory network (S1/M1, SMA, preSMA) was observed in all conducted tasks.

Leg movements in MARCOS were smooth with a maximum position error of 5 mm and a maximal force error of 20 N (Fig. 5).

In all conditions, brain activity was observed within a cluster covering post- and pre-central regions in the paracentral lobule (Fig. 6). The activity was restricted to the upper-leg/knee/lower-leg region within the human homunculus. The condition L-pas induced a large activity cluster covering right precuneus (BA5), postcentral areas (BA3) and primary/supplementary motor areas (BA4/6). Additionally, small clusters within the ipsilateral anterior cerebellar lobe and the right putamen were observed (not shown).

The condition R-pas induced a comparable activity cluster in contralateral hemisphere including the precuneus (BA5), postcentral (BA3) and motor primary/supplementary motor areas (BA4/6), whereas no activity was observed in the cerebellum.

L-act and R-act also induced activity within precuneal, postcentral and motor primary/supplementary motor areas. L-act additionally induced activity within ventral portions of the posterior cingulate.

Alt-pas and Alt-act induced activity patterns covering bilateral areas of the precuneus, sensory and motor/premotor regions. In comparison to Alt-pas, Alt-act induced stronger activity, reflected by a larger cluster.

Alt-pas-F and Alt act-F showed a more heterogenic picture. Both conditions induced less activity compared to the ones without application of foot sole force (Alt-pas/act).

Alt-pas-1 Hz induced again activity within precuneal, sensory and motor/premotor areas.

4. Discussion and conclusion

The MARCOS device allows assessing brain activity during gait-like stepping movements. The most important joint displacements (ankle, knee and hip) are included in these movements and contact forces can be applied to the foot sole, thus, imitating real gait conditions. Despite the challenging constraints posed by the scanner environment, both position and force can be controlled with high accuracy.

4.1. Influence on the MR environment

The temporal signal to noise ratio increased significantly only between the condition in which the device moved and the second base line scan. However, it was not possible to define a threshold for an acceptable difference. As the difference was quite small, and no difference to the first baseline scan was encountered, MARCOS was applied in a pilot study. Standard evaluation methods could be applied and the expected brain activity was found. Thus it is confirmed that the device had no considerable impact on image quality.

4.2. fMRI measurements

Head motion remained within a range that allowed meaningful data analysis and interpretation in almost all conditions. During the first 20 scans of task Alt-pas-F, the head drifted over 10 mm. For the following 140 scans, head motion remained in a range of below 2 mm.

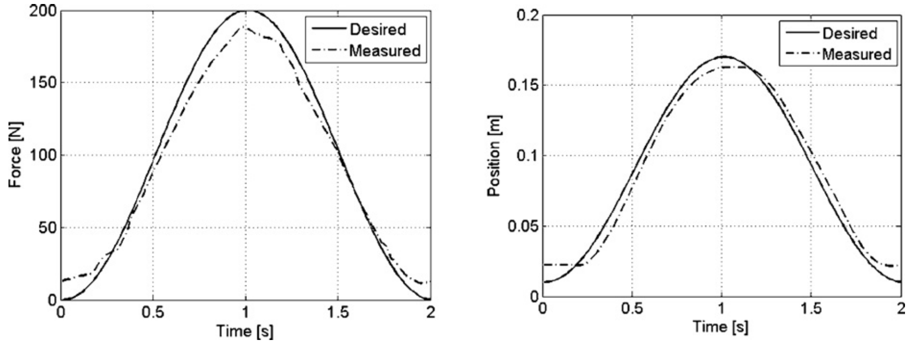

Fig. 5. Desired and measured trajectory of the subject's knee and forces at subject's feet during fMRI measurements with MARCOS.

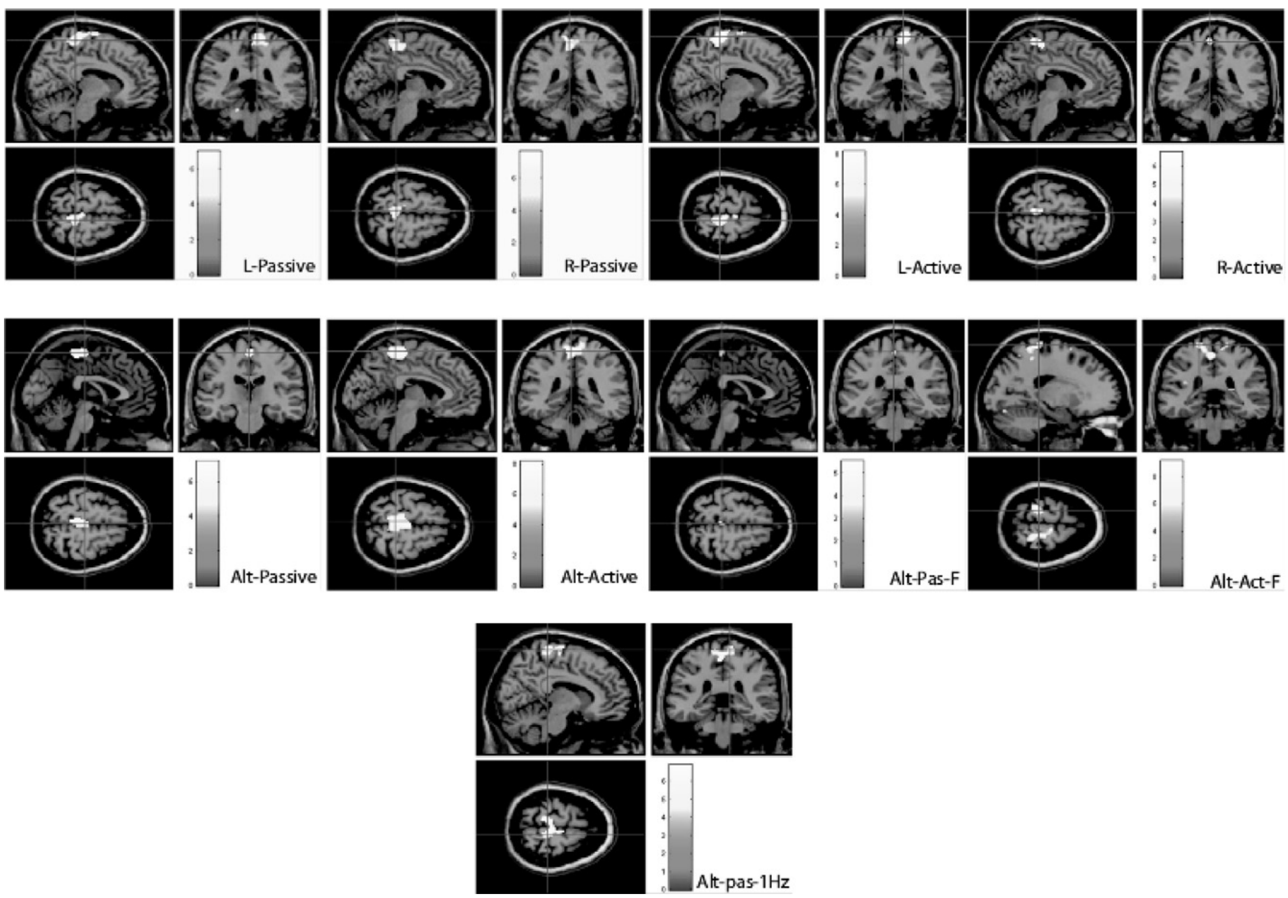

Fig. 6. Brain activity patterns of the single subject during all tasks. Depicted is a section in which the maximal activated voxel has been identified. Activity clusters were projected onto the T1_single_subject template, implemented in SPM8 with a conservative statistical threshold (FWE corrected, $p < 0.05$, 10 extended voxels).

According to the observed brain activity during the various experimental challenges, our hypotheses could be verified on single-subject basis: The more "uncommon" the motor task and the more "active" and "challenged" the subject was, the more activity was elicited within the sensorimotor brain areas. Activity was localized on the "core" centers of the sensorimotor network, specifically Brodman areas (BA3/4/5/6). Only the passive movement of the left leg induced activity within the cerebellum. No general conclusions about brain activity were drawn from the measurements as only a single subject was assessed. In conclusion, the present device can provide insight into human brain activity, while performing different gait-like leg movements in both active and passive modes. A significant foot loading could be applied by MARCOS, providing contact forces at the foot soles during stepping. This, in our opinion, is an important facet, as the sensory feedback of this specific force is of high relevance during walking (Dietz et al., 2002). Thus, MARCOS provides the opportunity to study the effects of essential cues of locomotion in healthy subjects and potentially in patients with movement disorders on brain activity. Therefore also therapeutic effects might reliably be assessed by this approach.

Further studies with healthy subjects are planned to investigate the impact of different foot loading and different stepping speeds on brain activity. Furthermore, patients suffering spinal cord and brain injuries will be included to elucidate brain activity due to a passive/active gait-like stepping movement as well as the effects of training on brain activity in order to optimize therapeutic protocols and approaches.

Acknowledgements

This work was supported by the EMDO Foundation, Koster Foundation, International Foundation of Paraplegia and the Swiss National Fonds. We thank Alessandro Rotta and Andreas Brunschweiler for support in crafting and assembling of MARCOS, and the Institute for Biomedical Engineering (ETH Zurich, Zurich, Switzerland) for their support and provision of scanning times.

References

Bakker M, de Lange FP, Stevens JA, Toni I, Bloem BR. Motor imagery of gait: a quantitative approach. Exp Brain Res 2007a;179:497–504.
Bakker M, Verstappen CCP, Bloem BR, Toni I. Recent advances in functional neuroimaging of gait. J Neural Transm 2007b;114:1323–31.
Bristow DA, Tharayil M, Alleyne AG. A survey of iterative learning control. Control Syst Mag IEEE 2006;26:96–114.
Christensen LOD, Johannsen P, Sinkjaer T, Petersen N, Pyndt HS, Nielsen JB. Cerebral activation during bicycle movements in man. Exp Brain Res 2000;135:66–72.
Ciccarelli O, Toosy AT, Marsden JF, Wheeler-Kingshott CM, Sahyoun C, Matthews PM, et al. Identifying brain regions for integrative sensorimotor processing with ankle movements. Exp Brain Res 2005;166:31–42.
Colombo G, Joerg M, Schreier R, Dietz V. Treadmill training of paraplegic patients using a robotic orthosis. J Rehabil Res Dev 2000;37:693–700.
Dietz V, Grillner S, Trepp A, Hubli M, Bolliger. Changes in spinal reflex and locomotor activity after a complete spinal cord injury: a common mechanism? Brain 2009;132:2196–205.
Dietz V, Duysens J. Significance of load receptor input during locomotion: a review. Gait Posture 2000;11:102–10.
Dietz V, Gollhofer A, Kleiber M, Trippel M. Regulation of bipedal stance: dependency on "load" receptors. Exp Brain Res 1992;89:229–31.
Dietz V, Muller R, Colombo G. Locomotor activity in spinal man: significance of afferent input from joint and load receptors. Brain 2002;125:2626–34.
Dobkin BH, Firestine A, West M, Saremi K, Woods R. Ankle dorsiflexion as an fMRI paradigm to assay motor control for walking during rehabilitation. NeuroImage 2004;23:370–81.
Firbank MJ, Coulthard A, Harrison RM, Williams ED. A comparison of two methods for measuring the signal to noise ratio on MR images. Phys Med Biol 1999;44:N261–4.
Fukuyama H, Ouchi Y, Matsuzaki S, Nagahama Y, Yamauchi H, Ogawa M, et al. Brain functional activity during gait in normal subjects: a SPECT study. Neurosci Lett 1997;228:183–6.
Hanakawa T, Katsumi Y, Fukuyama H, Honda M, Hayashi T, Kimura J, et al. Mechanisms underlying gait disturbance in Parkinson's disease—a single photon emission computed tomography study. Brain 1999;122:1271–82.
Ivanenko YP, Grasso R, Macellari V, Lacquaniti F. Control of foot trajectory in human locomotion: role of ground contact forces in simulated reduced gravity. J Neurophysiol 2002;87:3070–89.
Jahn K, Deutschlander A, Stephan T, Strupp M, Wiesmann M, Brandt T. Brain activation patterns during imagined stance and locomotion in functional magnetic resonance imaging. NeuroImage 2004;22:1722–31.
Kamibayashi K, Nakajima T, Takahashi M, Akai M, Nakazawa K. Facilitation of corticospinal excitability in the tibialis anterior muscle during robot-assisted passive stepping in humans. Eur J Neurosci 2009;30:100–9.
Kawashima N, Nozaki D, Abe MO, Akai M, Nakazawa K. Alternate leg movement amplifies locomotor-like muscle activity in spinal cord injured persons. J Neurophysiol 2005;93:777–85.
la Fougère C, Zwergal A, Rominger A, Förster S, Fesl G, Dieterich M, et al. Real versus imagined locomotion: a [18F]-FDG PET-fMRI comparison. NeuroImage 2010;50:1589–98.
Luft AR, Forrester L, Macko RF, McCombe-Waller S, Whitall J, Villagra F, et al. Brain activation of lower extremity movement in chronically impaired stroke survivors. NeuroImage 2005;26:184–94.
Luft AR, Smith GV, Forrester L, Whitall J, Macko RF, Hauser T-K, et al. Comparing brain activation associated with isolated upper and lower limb movement across corresponding joints. Hum Brain Map 2002;17:131–40.
MacIntosh BJ, Mraz R, Baker N, Tam F, Staines WR, Graham SJ. Optimizing the experimental design for ankle dorsiflexion fMRI. NeuroImage 2004;22:1619–27.
Malouin F, Richards CL, Jackson PL, Dumas F, Doyon J. Brain activations during motor imagery of locomotor-related tasks: a PET study. Hum Brain Map 2003;19:47–62.
Mehta JP, Verber MD, Wieser JA, Schmit BD, Schindler-Ivens SM. A novel technique for examining human brain activity associated with pedaling using fMRI. J Neurosci Methods 2009;179:230–9.
Miyai I, Suzuki M, Hatakenaka M, Kubota K. Effect of body weight support on cortical activation during gait in patients with stroke. Exp Brain Res 2006;169:85–91.
Miyai I, Tanabe HC, Sase I, Eda H, Oda I, Konishi I, et al. Cortical mapping of gait in humans: a near-infrared spectroscopic topography study. NeuroImage 2001;14:1186–92.
Perry J, Thorofare S, Davids JR. Gait analysis: normal and pathological function. J Pediatr Orthop 1992;12:815.
Sahyoun C, Floyer-Lea A, Johansen-Berg H, Matthews PM. Towards an understanding of gait control: brain activation during the anticipation, preparation and execution of foot movements. NeuroImage 2004;21:568–75.
Yu N, Gassert R, Riener R. Mutual interferences and design principles for mechatronic devices in magnetic resonance imaging. Int J Comput Assist Radiol Surg 2011;6:473–88.
Yu N, Hollnagel C, Blickenstorfer A, Kollias S, Riener R. Comparison of MRI-compatible mechatronic systems with hydrodynamic and pneumatic actuation. Mechatronics IEEE/ASME Trans 2008.